Determining the Structure of a Hydroxylase Enzyme That Catalyzes the Conversion of Methane to Methanol in Methanotrophic Bacteria

AMY C. ROSENZWEIG AND STEPHEN J. LIPPARD*

Department of Chemistry, Massachusetts Institute of Technology, Cambridge, Massachusetts 02139

Received March 1, 1994

Non-heme dinuclear iron centers linked by a monoatomic bridge and one or two carboxylate groups carry out a variety of biological functions that begin to rival those of the better known heme iron proteins.[1-4] Included are hemerythrin (Hr),[5] the R2 protein of ribonucleotide reductase (RR),[6,7] and the hydroxylase of methane monooxygenase (MMOH). In each of these proteins, the diiron core has a different function.[2] In Hr it binds O_2 reversibly, in the R2 protein it reacts with dioxygen to generate a tyrosyl radical involved in the reduction of ribonucleoside to deoxyribonucleoside diphosphates for DNA synthesis, and in MMOH it activates dioxygen for converting methane to methanol. Despite this functional diversity, the physical properties of the dinuclear iron sites in these proteins are very similar. The ability of one unit to serve so many different functions inspired us to study both carboxylate-bridged diiron model compounds and proteins.[4] In 1987, we began a research effort to investigate the soluble, diiron-containing MMOH from the methanotrophic bacterium *Methylococcus capsulatus* (Bath). This latter work is the focal point of the present Account.

Methanotrophic bacteria utilize methane as their sole source of carbon and energy,[8] converting it to methanol in the first step of their metabolic pathway (eq 1). The existence of methanotrophic bacteria has

$$CH_4 + NADH + H^+ + O_2 \rightarrow CH_3OH + NAD^+ + H_2O \quad (1)$$

been documented since the beginning of the century,[9] but it was not until the pioneering work of Whittenbury in the late 1960s and early 1970s[10,11] that pure cultures of these bacteria were made available in large quantities. In recent years, the role of methane in global warming,[12] the need for more efficient use of methane as an energy source,[13] and the potential use of methanotrophs for bioremediation of land[14,15] and water[16,17] have motivated study of these microorganisms as well as detailed investigations of MMO, the enzyme system responsible for the conversion of methane to methanol.

Soluble MMO from *M. capsulatus* (Bath), the first system to be purified,[18] consists of three proteins, a reductase (MW 38.6 kDa), also called protein C, a small coupling protein (MW 15.5 kDa), known also as protein B, and a hydroxylase (MW 251 kDa), formerly called protein A. All three proteins are necessary for enzyme activity. The MMO from *Methylosinus trichosporium* OB3b has also been purified[19,20] and is very similar to the *M. capsulatus* system. An MMO consisting of the hydroxylase and the reductase, but apparently lacking the coupling protein, has been isolated from *Methylobacterium* CRL-26.[21] In all systems, the reductase transfers electrons to the hydroxylase by means of its two prosthetic groups, a 2Fe–2S cluster and one FAD.[22] The coupling protein is a small polypeptide with no metal or prosthetic group[23] having several regulatory roles. The hydroxylase, which belongs to the growing class of functionally diverse carboxylate-bridged diiron proteins mentioned above, is the site of methane oxidation. As such, it is

Amy C. Rosenzweig received a B.A. degree (1988) in chemistry from Amherst College, where she was introduced to bioinorganic chemistry in the laboratory of Professor David M. Dooley. She received her Ph.D. degree (1994) from MIT, where she worked under the direction of Professor Stephen J. Lippard on the structural characterization of the methane monooxygenase hydroxylase. She is currently a postdoctoral fellow at Harvard Medical School, studying the methane monooxygenase components by X-ray crystallography with Professor Christin A. Frederick.

Stephen J. Lippard did his undergraduate work at Haverford College (B.A., 1962) and his graduate studies at MIT (Ph.D., 1965). He was a member of the Columbia University Chemistry Department until he returned to MIT (1982), where he is now the Arthur Amos Noyes Professor of Chemistry. His research interests span the fields of inorganic chemistry and biology, with current emphasis on non-heme iron proteins and models, platinum anticancer drugs, and ligand control of chemical reactivity in transition metal complexes. He recently coauthored a book entitled *Principles of Bioinorganic Chemistry* with Jeremy M. Berg.

(1) Sanders-Loehr, J. In *Iron Carriers and Iron Proteins*: VCH Publishers, Inc.: New York, 1989; pp 373–466.
(2) Vincent, J. B.; Olivier-Lilley, G. L.; Averill, B. A. *Chem. Rev.* **1990**, *90*, 1447–1467.
(3) Que, L., Jr.; True, A. E. *Prog. Inorg. Chem.* **1990**, *38*, 97–200.
(4) Lippard, S. J. *Angew. Chem., Int. Ed. Engl.* **1988**, *27*, 344–361.
(5) Stenkamp, R. E.; Sieker, L. C.; Jensen, L. H. *Nature* **1981**, *291*, 262–264.
(6) Nordlund, P.; Sjöberg, B.-M.; Eklund, H. *Nature* **1990**, *345*, 593–598.
(7) Nordlund, P.; Eklund, H. *J. Mol. Biol.* **1993**, *231*, 123–164.
(8) Anthony, C. *The Biochemistry of Methylotrophs*; Academic Press: New York, 1982; pp 296–379.
(9) Whittenbury, R.; Dalton, H. In *The Procaryotes*; Starr, M. P., Stolp, H., Truper, H. G., Balowes, A., Schlegel, H. G., Eds.; Springer-Verlag: Berlin, 1981.
(10) Whittenbury, R.; Phillips, K. C.; Wilkinson, J. F. *J. Gen. Microbiol.* **1970**, *61*, 205–218.
(11) Whittenbury, R.; Davies, S. I.; Davey, J. F. *J. Gen. Microbiol.* **1970**, *61*, 219–226.
(12) Lelieveld, J.; Crutzen, P. J.; Brühl, C. *Chemosphere* **1993**, *26*, 739–768.
(13) Periana, R. A.; Taube, D. J.; Evitt, E. R.; Löffler, D. G.; Wentrcek, P. R.; Voss, G.; Masuda, T. *Science* **1993**, *259*, 340–343.
(14) Lindstrom, J. E.; Prince, R. C.; Clark, J. C.; Grossman, M. J.; Yeager, T. R.; Braddock, J. F.; Brown, E. J. *Appl. Environ. Microbiol.* **1991**, *57*, 2514–2522.
(15) Pritchard, P. H.; Costa, C. F. *Environ. Sci. Technol.* **1991**, *25*, 372–379.
(16) Green, J.; Dalton, H. *J. Biol. Chem.* **1989**, *264*, 17698–17703.
(17) Fox, B. G.; Borneman, J. G.; Wackett, L. P.; Lipscomb, J. D. *Biochemistry* **1990**, *29*, 6419–6427.
(18) Colby, J.; Dalton, H. *Biochem. J.* **1978**, *171*, 461–468.
(19) Fox, B. G.; Lipscomb, J. D. *Biochem. Biophys. Res. Commun.* **1988**, *154*, 165–170.
(20) Fox, B. G.; Froland, W. A.; Dege, J. E.; Lipscomb, J. D. *J. Biol. Chem.* **1989**, *264*, 10023–10033.
(21) Patel, R. N.; Savas, J. C. *J. Bacteriol.* **1987**, *169*, 2313–2317.
(22) Lund, J.; Dalton, H. *Eur. J. Biochem.* **1985**, *147*, 291–296.
(23) Green, J.; Dalton, H. *J. Biol. Chem.* **1985**, *260*, 15795–15801.

0001-4842/94/0127-0229$04.50/0

the key component in the enzyme system. MMOH is a multimeric protein having two copies each of three different subunits; the holoenzyme is $\alpha_2\beta_2\gamma_2$ (α, MW 60.6 kDa; β, MW 45 kDa; γ, MW 19.8 kDa).[24] We have recently solved the X-ray structure of MMOH at 2.2-Å resolution.[25]

Our purpose in this Account is to review the structural work on the hydroxylase carried out by ourselves and others in the context of the now known X-ray structure. We address the question, How well did the noncrystallographic methods reveal key features of the protein structure? Of particular interest were the following questions: (1) What is the structure of the holoenzyme, and how do the three subunits interact? (2) How many diiron centers are present, and which subunit(s) accommodate(s) them? (3) What exogenous and endogenous species are coordinated to the diiron center, and what specific amino acid residues serve as ligands? (4) How does the hydroxylase interact with the other two MMO proteins? We begin by discussing spectroscopic and biochemical data obtained with methodologies other than X-ray crystallography and the resulting models pertaining to each of the foregoing structural questions. We then briefly discuss the X-ray determination and conclude by comparing the known structure to the models derived from the noncrystallographic experiments.

Noncrystallographic Approaches

Holo Hydroxylase and Subunit Interactions. In the first reported purification of the *M. capsulatus* hydroxylase,[24] three subunits of molecular weights 54, 42, and 17 kDa were identified by SDS polyacrylamide gel electrophoresis (PAGE). They were determined to be present in equimolar quantities by densitometric analysis. Since the total molecular weight was 210 kDa by gel filtration and 253 kDa by nondenaturing PAGE, it was concluded that there were two copies of each of the three subunits, an $\alpha_2\beta_2\gamma_2$ arrangement. Similar results were later obtained for the *M. trichosporium* hydroxylase, the native molecular weight being 245 kDa by gel filtration and ultracentrifugation, with subunit molecular weights of 54, 43, and 23 kDa.[20] In addition, the subunit structure of the *Methylobacterium* CRL-26 hydroxylase was determined to be $\alpha_2\beta_2\gamma_2$ with molecular weights of 55, 40, and 20 kDa for the respective subunits and a total molecular weight of 220 kDa.[21]

The cloning of a 12-kb *Eco*R1 genomic DNA restriction fragment encoding all three subunits and the reductase as well as two open reading frames, *orfX* and *orfY*, revealed the genes to be contiguous in the *M. capsulatus* genome, forming an MMO operon.[26] The sequences of the three subunits (α, *mmoX*; β, *mmoY*; γ, *mmoZ*) and of the reductase (*mmoC*) were identified,[27] and one of the open reading frames (ORFs), *orfY*, was subsequently proved to be the gene for the coupling protein.[28,29] The availability of these sequences was essential for the X-ray structure determination. The MMO genes for the *M. trichosporium* hydroxylase have also been cloned,[30] and the two hydroxylases are homologous with 80% identity for the α subunit, 59% identity for the β subunit, and 49% identity for the γ subunit. There are slightly different numbers of amino acid residues in the α, β, γ subunits from the two different hydroxylases, with 527 (525), 389 (394), and 170 (169) residues for the *M. capsulatus* (*M. trichosporium*) enzymes, respectively.

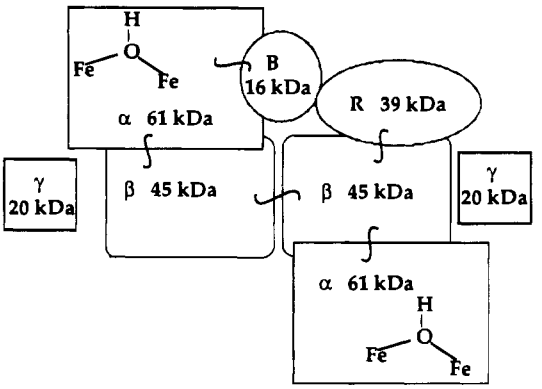

Figure 1. Postulated arrangement of hydroxylase subunits and components of the MMO hydroxylase based on chemical cross-linking experiments.[33] The coupling protein is labeled B, and the reductase, R.

Very little information pertaining to the secondary structure of the hydroxylase was available. On the basis of alignments of the sequence of the α subunit with the ribonucleotide reductase R2 protein, it was suggested that the diiron center is situated in a four-helix bundle.[31] In addition, circular dichroism spectra of the *M. capsulatus* hydroxylase suggested a high helical content.[32] The only model for the arrangement of the three subunits was derived from chemical cross-linking experiments with the *M. trichosporium* hydroxylase.[33] Reaction of the hydroxylase with the covalent cross-linking reagent 1-ethyl-3-(3-(dimethylamino)propyl)carbodiimide (EDC) resulted in several products, two of which were identified as cross-linked α and β subunits and a dimer of β subunits. No cross-linking of the γ subunit was observed, even in the presence of the cross-linking catalyst *N*-hydroxysulfosuccinimide. Since EDC is a zero-length cross-linking reagent, the sites of attachment correspond to sites of inter-subunit salt bridges. The subunit arrangement inferred from these experiments is shown in Figure 1.

Number and Location of Dinuclear Iron Centers. The presence of a dinuclear iron center similar to those found in hemerythrin and the R2 protein was first revealed by EPR studies of the *M. capsulatus* hydroxylase. In these experiments, dithionite-reduced samples exhibited a $g < 2$ signal typical of a dinuclear $Fe^{II}Fe^{III}$ center.[34] A similar signal, with $g_{av} = 1.85$, was subsequently observed for the *M. trichosporium*,[20]

(24) Woodland, M. P.; Dalton, H. *J. Biol. Chem.* **1984**, *259*, 53–59.
(25) Rosenzweig, A. C.; Frederick, C. A.; Lippard, S. J.; Nordlund, P. *Nature* **1993**, *366*, 537–543.
(26) Stainthorpe, A. C.; Murrell, J. C.; Salmond, G. P. C.; Dalton, H.; Lees, V. *Arch. Microbiol.* **1989**, *152*, 154–159.
(27) Stainthorpe, A. C.; Lees, V.; Salmond, G. P. C.; Dalton, H.; Murrell, J. C. *Gene* **1990**, *91*, 27–34.
(28) Pilkington, S. J.; Salmond, G. P. C.; Murrell, J. C.; Dalton, H. *FEMS Microbiol. Lett.* **1990**, *72*, 345–348.
(29) Rosenzweig, A. C.; Feng, X.; Lippard, S. J. In *IUCCP Symposium on Applications of Enzyme Biotechnology*; Kelly, J. W., Baldwin, T. O., Eds.; Plenum Press: New York, 1991.
(30) Cardy, D. L. N.; Salmond, G. P. C.; Murrell, J. C. *Mol. Microbiol.* **1991**, *5*, 335–342.
(31) Nordlund, P.; Dalton, H.; Eklund, H. *FEBS Lett.* **1992**, *307*, 257–262.
(32) Smith, D. D. S.; Dalton, H. *Eur. J. Biochem.* **1992**, *210*, 629–633.
(33) Fox, B. G.; Liu, Y.; Dege, J. E.; Lipscomb, J. D. *J. Biol. Chem.* **1991**, *266*, 540–550.
(34) Woodland, M. P.; Patil, D. S.; Cammack, R.; Dalton, H. *Biochim. Biophys. Acta* **1986**, *873*, 237–242.

Methylobacterium CRL-26, and *Methylococcus* CRL-25 hydroxylases.[35] Upon further reduction, a broad resonance at $g = 16$, characteristic of the even spin $Fe^{II}Fe^{II}$ state, was identified for both the *M. trichosporium*[36] and *M. capsulatus*[37] hydroxylases. Initial reports of 2 Fe per $\alpha_2\beta_2\gamma_2$ hydroxylase dimer for the *M. capsulatus* hydroxylase[24] were subsequently revised upward when reconstitution of the apoenzyme increased the specific activity and raised the iron content to 3.3 Fe per protein.[38] A value of 2.8 Fe per dimer has been reported for the *Methylobacterium* CRL-26 protein.[21] For the *M. trichosporium* hydroxylase, an iron content of 4 per dimer and higher specific activities were obtained, results that were attributed to the use of Fe and cysteine in the purification buffers.[20] In our purifications of the *M. capsulatus* protein, we usually observe 2–3 Fe atoms per protein molecule, with occasionally higher values, and derived no benefit from including Fe and cysteine in the purification buffers.[37] In a very recent investigation, the *M. capsulatus* hydroxylase was depleted of Fe by using 3,4-dihydroxybenzaldehyde and then reconstituted with Mn(II) ions. The incorporation of just two Mn(II) ions was quantitated by EPR spectroscopy, and it was concluded that the *M. capsulatus* hydroxylase contains just one diiron site.[39]

Several lines of evidence suggested that the diiron center(s) is located on the α subunit. Reactions of the hydroxylase with [^{14}C]acetylene, a suicide substrate, led to incorporation of the radiolabel into the α subunit, indicating that it contains the catalytically active center.[40] Additional evidence that the diiron center resides in the α subunit comes from EPR and cross-linking studies. The EPR spectrum of the mixed-valent hydroxylase was perturbed by addition of the coupling protein,[33] suggesting that it binds near the diiron center. Cross-linking experiments yielded a covalent attachment between the α subunit and coupling protein, which did not form cross-links to any other subunits.[33]

The Bridging Ligands. The nature of the bridging ligands in the hydroxylase diiron core was investigated by a variety of spectroscopic techniques. Both the *M. capsulatus* and *M. trichosporium* hydroxylases are essentially colorless, with no optical bands beyond 300 nm.[20,37] Oxo-bridged diiron(III) proteins and model complexes typically exhibit absorption features in the 300–800-nm range.[3] A peak at 410 nm was observed for the *Methylobacterium* CRL-26 hydroxylase,[21] but we have shown that such a feature is most likely due to a cytochrome impurity.[37]

Hemerythrin and the R2 protein both display resonance Raman bands attributable to an Fe–O–Fe symmetric stretch, but no such Raman feature has been observed for the native hydroxylase. Moreover, preliminary EXAFS studies of the *M. capsulatus* and *M. trichosporium* hydroxylases indicated the absence of an oxo bridge. For these samples, which were photoreduced to the mixed-valence redox state in the X-ray beam, the short Fe–O distance (~1.8 Å) typically associated with an Fe–O–Fe unit was not observed.[41] The EXAFS data instead were similar to those for the hydroxo-bridged model compound, $[Fe_2(OH)(OAc)_2(HB(pz)_3)_2](ClO_4)$.[42] In a more detailed EXAFS analysis, Fe···Fe distances of 3.42 Å were determined for both the diferric and mixed-valence hydroxylases. This value indicated the presence of a monoatomic and at least one additional bridging ligand. The distance between the iron atoms and the monoatomic bridge is too long for it to be an oxo ligand, but is consistent with an assignment as hydroxide, monodentate carboxylate, or alkoxide.[37] An EXAFS study of the *Methylobacterium* CRL-26 hydroxylase yielded an Fe···Fe distance of 3.05 Å,[35] a discrepancy that may be due to differences in analysis protocol.[37] In this work, no evidence pertaining to the presence or absence of a short Fe–O distance was reported.

Antiferromagnetic coupling constants of $J = -32$ cm^{-1} for the mixed-valence *M. capsulatus*[37] and $J = -30$ cm^{-1} for the *M. trichosporium*[33] hydroxylase proteins were also measured by power saturation EPR experiments, where $H = -2J\mathbf{S}_1\cdot\mathbf{S}_2$. These values are also consistent with the presence of monoatomic hydroxo, carboxylato, or alkoxo bridges. A J value of -8 cm^{-1} has recently been determined for the diferric *M. trichosporium* hydroxylase.[43] Finally, the Mössbauer spectroscopic parameters for both hydroxylases fall in between values for oxo- and hydroxo-bridged model compounds and are therefore of little value in revealing the nature of the monoatomic bridging ligand.[37] From the accumulated data, we concluded that the oxidized hydroxylase does not contain an oxo bridge, but that hydroxo, alkoxo, and monodentate carboxylate bridges were reasonable candidates. The nature of the monoatomic bridge in the diiron center was finally resolved by a proton ENDOR study of the mixed-valence *M. capsulatus* hydroxylase.[44] A set of exchangeable resonances with $A \sim 14$–30 MHz detected in the proton ENDOR spectrum were strikingly similar to resonances seen for semimet azidohemerythrin, and attributed to the hydroxo bridge in that protein. The hydroxylase resonances were therefore assigned to a bridging hydroxide. Since the EXAFS showed similar Fe···Fe distances for the mixed-valence and oxidized hydroxylases, it was further concluded that a hydroxo bridge is probably present in the oxidized hydroxylase as well. Related experiments were subsequently reported for the mixed-valence *M. trichosporium* hydroxylase,[45] from which it was similarly concluded that hydroxide ion is the monoatomic bridge.

(35) Prince, R. C.; George, G. N.; Savas, J. C.; Cramer, S. P.; Patel, R. N. *Biochim. Biophys. Acta* **1988**, *952*, 220–229.
(36) Hendrich, M. P.; Münck, E.; Fox, B. G.; Lipscomb, J. D. *J. Am. Chem. Soc.* **1990**, *112*, 5861–5865.
(37) DeWitt, J. G.; Bentsen, J. G.; Rosenzweig, A. C.; Hedman, B.; Green, J.; Pilkington, S.; Papaefthymiou, G. C.; Dalton, H.; Hodgson, K. O.; Lippard, S. J. *J. Am. Chem. Soc.* **1991**, *113*, 9219–9235.
(38) Green, J.; Dalton, H. *J. Biol. Chem.* **1988**, *263*, 17561–17565.
(39) Atta, M.; Fontecave, M.; Wilkins, P. C.; Dalton, H. *Eur. J. Biochem.* **1993**, *217*, 217–223.
(40) Prior, S. D.; Dalton, H. *FEMS Microbiol. Lett.* **1985**, *29*, 105–109.
(41) Ericson, A.; Hedman, B.; Hodgson, K. O.; Green, J.; Dalton, H.; Bentsen, J. G.; Beer, R. H.; Lippard, S. J. *J. Am. Chem. Soc.* **1988**, *110*, 2330–2332.
(42) Armstrong, W. H.; Lippard, S. J. *J. Am. Chem. Soc.* **1984**, *106*, 4632–4633.
(43) Fox, B. G.; Hendrich, M. P.; Surerus, K. K.; Andersson, K. K.; Froland, W. A.; Lipscomb, J. D.; Münck, E. *J. Am. Chem. Soc.* **1993**, *115*, 3688–3701.
(44) DeRose, V.; Liu, K. E.; Lippard, S. J.; Hoffman, B. *J. Am. Chem. Soc.* **1993**, *115*, 6440–6441.
(45) Thomann, H.; Bernardo, M.; McCormick, J. M.; Pulver, S.; Andersson, K. K.; Lipscomb, J. D.; Solomon, E. I. *J. Am. Chem. Soc.* **1993**, *115*, 8881–8882.

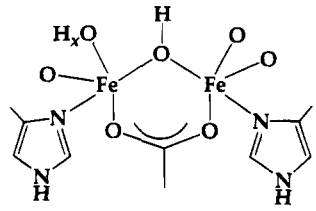

Figure 2. Model of the coordination sphere of the diiron(III) center in the MMO hydroxylase based on combined spectroscopic and biochemical information.

The Nonbridging Ligands. Some information about the nature of the nonbridging ligands in the diiron core was also obtained from spectroscopic experiments. According to the EXAFS data, the average first-shell coordination consists of 5–6 oxygen or nitrogen ligands at distances of 2.04 Å for the diferric hydroxylase, 2.06–2.08 Å for the mixed-valence hydroxylase, and 2.15 Å for the fully reduced hydroxylase. For the diferric R2 protein, which has just two coordinated histidines, the average first-shell coordination distance is 2.04–2.06 Å, whereas for oxyhemerythrin, which has five capping histidines, the average first-shell coordination distance is 2.15 Å.[2] These values suggested that, like the R2 protein, the hydroxylase contains more oxygen than nitrogen donor ligands. The presence of histidine nitrogen ligands in the mixed-valence hydroxylase was further investigated by ESEEM and ENDOR spectroscopies. The ESEEM spectrum of the *M. capsulatus* hydroxylase revealed the presence of histidine ligands coordinated to each of the different Fe atoms.[46] In addition, ^{14}N ENDOR spectroscopy demonstrated the presence of one or more coordinated histidines in the *M. trichosporium* hydroxylase.[47] Chemical modification of the oxidized *M. capsulatus* hydroxylase with diethyl pyrocarbonate, which reacts with histidine residues, showed that, in the apo hydroxylase, 14 histidines were reactive, but in the iron-containing hydroxylase, only 12 histidines could be modified, suggesting that two histidines are ligated to the diiron center.[32] Finally, a coordinated water molecule or hydroxide was identified in the proton ENDOR spectrum of the mixed-valence hydroxylase.[44,45] A model of the diiron center based on these combined spectroscopic and biochemical data is shown in Figure 2.

Specific Amino Acid Residues in the Active Site. At this point, a working model of the diiron core structure had been developed, but no information about the specific amino acid residues present in the active site was yet available. Several alignments of the amino acid sequence of the α subunit of the hydroxylase, believed to contain the diiron center for the reasons indicated above, with that of the R2 subunit of ribonucleotide reductase were proposed.[27,31] In the most detailed model,[31] depicted in Figure 3, the sequence of the α subunit was aligned with the iron-coordinating four-helix bundle of the R2 protein. This alignment suggested that Glu114, Glu144, His147, Glu209, Glu243, and His246 are coordinated to the iron atoms, and that other specific residues, including Ile239, Ile217, and Thr213, are present in the active site pocket. Notably, in the hydroxylase, cysteine

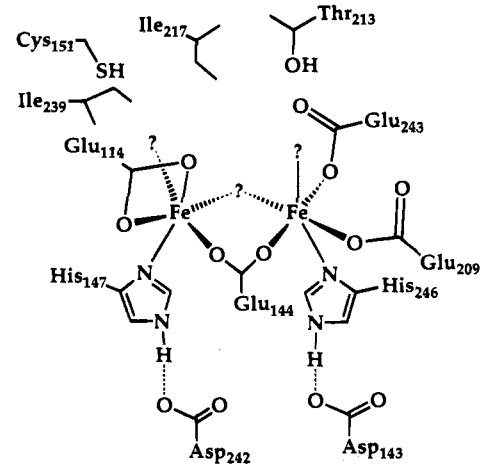

Figure 3. Proposed structure of the diiron(III) center in the MMO hydroxylase α subunit based on gene sequence homology with the R2 protein of ribonucleotide reductase.[31]

residue Cys151 was postulated to replace the functionally important tyrosyl radical site Tyr122 found in the R2 protein. Although this model could not provide exact details of coordination, the presence of two coordinated histidines and several oxygen ligands was consistent with the spectroscopic data. For the *M. trichosporium* hydroxylase, Glu209 is replaced by an aspartic acid residue, according to the gene sequence.[30]

Interactions with the Coupling Protein and the Reductase. As mentioned above, the coupling protein perturbs the EPR spectrum of the mixed-valence hydroxylase and can be cross-linked to the α subunit. In addition, the EXAFS spectra of the mixed-valence hydroxylase show slight differences in the presence of the coupling protein.[48] The coupling protein regulates electron transfer by helping to tune the redox potentials of the diiron center in both the *M. capsulatus* and *M. trichosporium* hydroxylases.[49,50] The coupling protein also affects the rate and regioselectivity of substrate oxidation.[51,52] Taken together, these data indicate that the coupling protein induces some sort of conformational change near the substrate binding site and diiron center. It is therefore placed proximal to the α subunit in the model shown in Figure 1.

The reductase neither affects the diiron center nor changes the rate or regioselectivity of substrate oxidation, and covalent attachment of this component and the β subunit was observed in the chemical cross-linking experiments.[33] If the binding domain for the reductase lies on the β subunit and the diiron center is located on the α subunit, it is unlikely, although not impossible, that the reductase would change the spectroscopic properties of the diiron center. Complexes between the reductase and the hydroxylase and the reductase and the coupling protein have been detected by fluorescence spectroscopy.[33] In the pres-

(46) Bender, C.; Rosenzweig, A. C.; Lippard, S. J.; Peisach, J. *J. Biol. Chem.*, in press.
(47) Hendrich, M. P.; Fox, B. G.; Andersson, K. K.; Debrunner, P. G.; Lipscomb, J. D. *J. Biol. Chem.* **1992**, *267*, 261–269.
(48) DeWitt, J. G.; Rosenzweig, A. C.; Hedman, B.; Lippard, S. J.; Hodgson, K. O. Manuscript in preparation.
(49) Liu, K. E.; Lippard, S. J. *J. Biol. Chem.* **1991**, *266*, 12836–12839.
(50) Paulsen, K. E.; Liu, Y.; Fox, B. G.; Lipscomb, J. D.; Münck, E.; Stankovich, M. T. *Biochemistry* **1994**, *33*, 713–722.
(51) Liu, K. E.; Feig, A. L.; Goldberg, D. P.; Watton, S. P.; Lippard, S. J. In *The Activation of Dioxygen and Homogeneous Catalytic Oxidation*; Barton, D. H. R., Martell, A. E., Sawyer, D., Eds.; Plenum Press: New York, 1993.
(52) Froland, W. A.; Andersson, K. K.; Lee, S.-K.; Liu, Y.; Lipscomb, J. D. *J. Biol. Chem.* **1992**, *267*, 17588–17597.

ence of the reductase, the tryptophan fluorescence of the hydroxylase is quenched by 86%, and that of the coupling protein by 78%. In addition, a shift in the fluorescence maximum is observed for the coupling protein complexed with the reductase. These observations suggest that the binding domains for the coupling protein and the reductase, although residing on different subunits, are arranged in such a way that these components can interact with one another (Figure 1).

Structural Information from X-ray Crystallography

Brief History of the X-ray Structure Determination. Since a complete structural characterization of the hydroxylase ultimately requires a three-dimensional X-ray analysis, we initiated attempts to crystallize the enzyme in mid-1990 in collaboration with Professor C. A. Frederick of Harvard Medical School. After >1000 crystallization trials, we obtained thin crystalline plates that diffracted to better than 2.2-Å resolution. The first diffraction patterns, observed in May 1991, gave unit cell dimensions of 62.6 × 110.1 × 333.5 Å and the orthorhombic space group $P2_12_12_1$.[53] The long cell dimension of 333.5 Å posed a frustrating problem in data collection because the imaging plate detector available to us had limited spatial resolution, allowing recording of data to just 3.5-Å resolution. In addition, the thin crystal size made it difficult to collect good quality data with conventional laboratory X-ray sources. Both of these problems were overcome by the use of synchrotron radiation. We collected 3.0-Å native data and several partial heavy atom derivative data sets to 3.7-Å resolution at Stanford Synchrotron Radiation Laboratory (SSRL) in August 1992. The difference Patterson map for one of the heavy atom derivatives, PIP, bis-(μ-iodo)bis(ethylenediamine)diplatinum(II), collected at SSRL was solved, marking the first breakthrough in the structure determination. By using phases from the PIP derivative for difference Fourier maps, the heavy atom positions in several other derivatives were determined. These heavy atom sites led to the identification of a noncrystallographic 2-fold axis relating the two $\alpha\beta\gamma$ halves of the hydroxylase dimer. It was then possible to employ molecular averaging to improve our native multiple isomorphous replacement (MIR) electron density maps. After averaging, the 3.5-Å maps revealed some secondary structure elements, but interpretation of the structure was not possible without higher resolution data.

In December 1992, with our new collaborator Professor P. Nordlund of Stockholm University, we traveled to the Photon Factory in Tsukuba, Japan, where, with the kind assistance of Professor N. Sakabe, we collected a 2.2-Å native data set by using a modified Weissenberg camera with imaging plates. In February 1993, we collected a number of 3.0-Å derivative data sets at SSRL, and these derivative data sets and the 2.2-Å native data were used to calculate 3.0-Å native averaged maps of the hydroxylase, which were superior to the previous 3.5-Å maps. A hypothesis for the location of the diiron center was formulated from a native anomalous map and the presence of a mercury binding site, which we postulated to be the cysteine residue (Cys151) near the dinuclear iron center that had been predicted by the sequence alignment with the ribonucleotide reductase R2 protein mentioned above.[31] A sufficient number of helices were evident in the map to build the iron-coordinating four-helix bundle into the electron density map, thus defining part of the α subunit. We then pursued a strategy in which the MIR phases were gradually improved by the combination of phase information from a partial model. Eventually, the β and γ subunits were located, and their sequences were fit by using the heavy atom sites as markers for cysteine, histidine, or methionine residues.

Fitting the electron density to the known sequence for the α and γ subunits proceeded without problems once portions of the sequences were recognized. We encountered some difficulty, however, in fitting the last 30 residues in the C-terminus of the published sequence[26] for the β subunit to the electron density map. In particular, residue 363 was clearly a tryptophan, but the sequence had a glycine at this position. The addition of either one thymidine or one cytidine base at position 4227 in the *mmoY* gene sequence resulted in an appropriate frame shift, changing the GGA codon for Gly to TGG, which codes for Trp. The newly derived amino acid sequence was consistent with the electron density map and includes two more residues at the C-terminus, so that the β subunit now contains 389 rather than 387 residues (Trp 363-Ile-Glu-Asp-Tyr-Ala-Ser-Arg-Ile-Asp-Phe-Lys-Ala-Asp-Arg-Asp-Gln-Ile-Val-Lys-Ala-Val-Leu-Ala-Gly-Leu-Lys 389). The presence of an additional cytidine base at position 4227 was subsequently confirmed by gene sequencing.[54] When the new sequence is compared to that of the *M. trichosporium* β subunit, there are 11 identical residues in the C-terminal 30 residues, whereas, with the incorrect sequence, only four residues were conserved between the two species.

By the end of September 1993, we had a model which contained 512 of the 527 residues in the α subunit, 384 of the 389 residues in the β subunit, and 162 of the 170 residues in the γ subunit. There is no electron density for the first 15 residues in the α subunit, the first six residues in the β subunit, and the first residue and last seven residues in the γ subunit, all of which chain termini are presumably disordered in the crystal.[25]

X-ray Structure of the Hydroxylase. The X-ray structure of the holo hydroxylase, shown in Figure 4, confirms the presence of an $\alpha_2\beta_2\gamma_2$ polypeptide chain arrangement. The two $\alpha\beta\gamma$ protomers form a large heart, with the noncrystallographic 2-fold axis running down the opening in the center of the molecule. The protein secondary structure is primarily helical with just two small β hairpin structures in the α subunit. Whereas circular dichroism spectroscopic measurements had indicated a large amount of helical structure,[32] no detailed information could be obtained without an X-ray structure. Remarkably, 10 helices in each of the α and β subunits have identical folds, although there is no detectable primary sequence homology. This feature of the structure was completely unexpected. Furthermore, the folds of the α and β subunits resemble those of the ribonucleotide

(53) Rosenzweig, A. C.; Frederick, C. A.; Lippard, S. J. *J. Mol. Biol.* **1992**, *227*, 283–285.

(54) Coufal, D. E.; Lippard, S. J. Unpublished results.

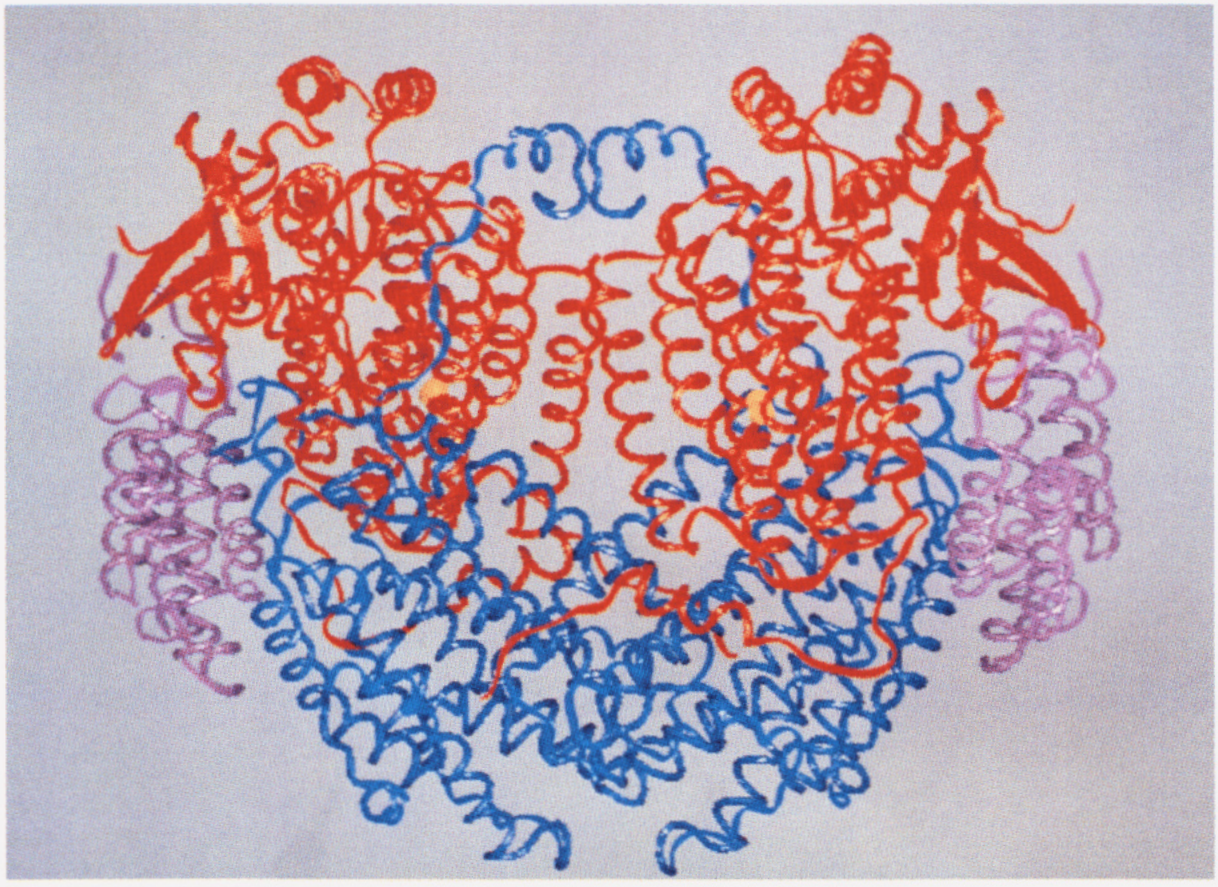

Figure 4. Structure of the hydroxylase as determined by X-ray crystallography.[25] The α subunits are shown in red, the β subunits in blue, and the γ subunits in violet. The iron atoms are represented as yellow spheres.

reductase R2 protein, also a surprise. Although the sequence alignment did suggest that the diiron center was located in the same kind of four-helix bundle present in the R2 protein,[31] the extent of the similarity between the structures was not anticipated.

The interaction between the two protomers, which we have designated A and B, is primarily between the two β subunits. Most of these interactions occur at the opening in the center of the hydroxylase dimer. By contrast, there are no inter-subunit salt linkages between the two α subunits. There are also several interactions between the α and β subunits. The γ subunit does not participate in the dimer interaction, but is associated with the α and β subunits through several Glu-Arg salt bridges. The observation of an αβ chemically cross-linked product[33] is consistent with the X-ray structure, having several Glu-Lys and Asp-Lys interactions which are good candidates for cross-linking by EDC. The cross-linking study failed to reveal products involving the γ subunit, however, probably because all the salt bridges formed by this subunit involve arginine residues. Whereas lysine residues can form stable cross-linked products, arginine residues have a high pK_a and are less likely to form a stable amide bond. A low-yield ββ cross-linked product was observed,[33] yet the interactions between the two β subunits also involve only arginine residues. The cross-linking experiments were carried out on the *M. trichosporium* hydroxylase, which might explain discrepancies between the cross-linking data and the X-ray structure if the two structures were different. This possibility seems unlikely, however, since every residue involved in inter-subunit interactions in the *M. capsulatus* hydroxylase is conserved in the *M. trichosporium* gene sequence. The predicted and actual relationships among the three subunits can be seen by comparing Figures 1 and 5, respectively.

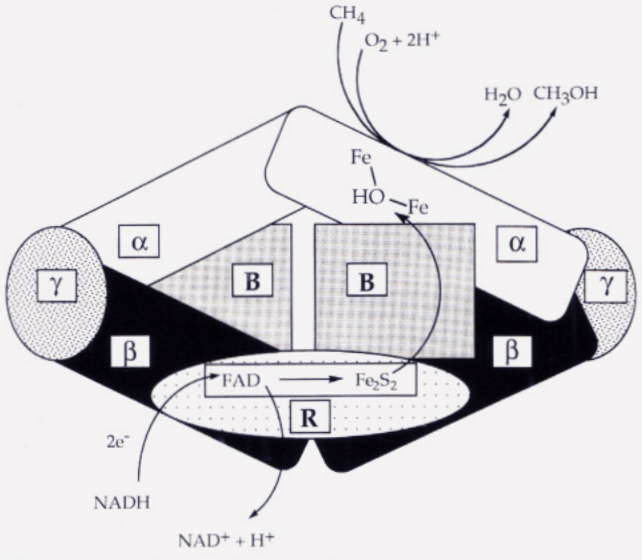

Figure 5. Scheme showing the known relationship among subunits in the hydroxylase from the X-ray structure determination and postulated component binding sites. Reprinted with permission from ref 57. Copyright 1994 American Chemical Society. A second reductase molecule, related by a C_2 symmetry axis to the one depicted, is not visible in this view.

The X-ray structure unambiguously shows that there are two diiron sites in the hydroxylase, one located on each α subunit, separated by 45 Å. The iron atoms in the hydroxylase structure are shown as spheres in Figure 4. The two sites appear to be fully

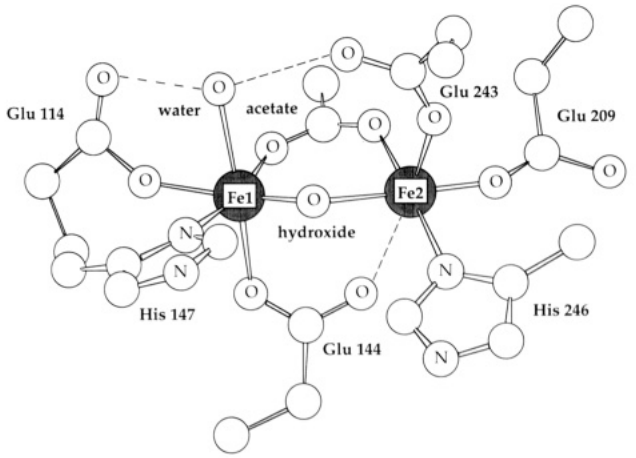

Figure 6. Structure of the dinuclear iron center in the oxidized hydroxylase as determined by X-ray crystallography.[25]

occupied.[25] The location of the diiron center is consistent with the chemical labeling and cross-linking experiments. As predicted by the alignment with the sequence of the R2 protein, the diiron center is positioned within a four-helix bundle, which donates the coordinating amino acid residues. The presence of four Fe atoms supports quantitative results reported for the *M. trichosporium* hydroxylase,[20] but contradicts our typically measured values of 2 Fe atoms and the reported reconstitution of the apo hydroxylase with 2 Mn(II) atoms.[39] It may be that we have crystallized a 4-Fe enzyme from a mixture of apoprotein and iron-depleted protein, and preliminary results in our laboratory indicate that an insoluble fraction of apoprotein can be removed from hydroxylase samples resulting in a higher Fe content.[55]

The X-ray structure of the hydroxylase reveals three ligands bridging the 2 Fe atoms (Figure 6). The two iron atoms are linked by one carboxylate ligand derived from the protein, Glu144. We have designated this carboxylate a "semibridging" ligand because the Fe−O distances for one of the Fe atoms, Fe2, of 2.5 and 2.7 Å in the two protomers, are longer than expected for normal iron(III)−carboxylate bonds. Although the carboxylate bridge was expected, this semibridging character was impossible to predict from any of the spectroscopic studies. In addition, two exogenous bridging ligands were apparent in the $|F_o| - |F_c|$ difference Fourier maps. We have assigned one of these ligands as a hydroxo bridge. For this assignment, we relied on the proton ENDOR data,[44] since we cannot distinguish among oxide, hydroxide, and water in the electron density map. Furthermore, the Fe···Fe distance is 3.4 Å in both protomers, a value consistent with a hydroxo bridge and in good agreement with the EXAFS data for the both the diferric and mixed-valence hydroxylases.[37] A comparison of the EXAFS and X-ray structures raises an additional question. Since the EXAFS samples were photoreduced to the mixed-valence form in the X-ray beam, it is possible that the crystals may have undergone a similar photoreduction, since the data were collected with synchrotron radiation. This possibility seems unlikely, however, since XAS edge studies of single crystals of the hydroxylase irradiated for much longer than those used in the X-ray determination showed no evidence for photoreduction to the mixed-valence form.[56] We have assigned a second exogenous bridging ligand as an acetate ion, the source of which is most likely ammonium acetate in the crystallization buffers. Bicarbonate ion was considered as an alternative assignment, but there are no hydrogen-bonding interactions to this ligand, which might be expected for such a species.

The nonbridging ligands in the diiron center comprise the amino acid residues suggested in the sequence alignment with the R2 protein.[31] As shown in Figure 6, Fe1 is coordinated to the δN atom of His147 and Fe2 to the δN atom of His246. Histidine ligands were predicted correctly by the ESEEM, ENDOR, and EXAFS experiments and by the sequence alignments. Fe1 is coordinated to one monodentate carboxylate, Glu114, and Fe2 is ligated to two monodentate carboxylates, Glu209 and Glu243. The presence of more oxygen than nitrogen ligands was suggested by the EXAFS analysis. The fact that all the nonbridging carboxylate ligands are monodentate was not previously determined. Finally, Fe1 is coordinated to a water molecule, a third exogenous ligand, as anticipated by the proton ENDOR data.[44] According to the ENDOR study, this ligand could be assigned as either a terminal water or hydroxide. The combination of a bridging hydroxide and a terminal water ligand renders the active site charge neutral, so we have chosen to assign this ligand as a water molecule. The fact that it forms hydrogen bonds with both Glu 114 and Glu 243 supports this assignment. Other residues present in the active site, which had not been identified by spectroscopic or biochemical methods, were also predicted accurately by the sequence alignment, including Cys151 and two aspartic acid residues, Asp242 and Asp143, which are hydrogen bonded to His147 and His246, respectively. The presence of Cys151 in the space occupied by the tyrosyl radical in the R2 protein suggests a redox role for this residue in the catalytic mechanism. One possible mechanism involving Cys151 has been described,[57] but currently, there are no experimental data which either support or disprove such a mechanism.

The X-ray structure reveals possible binding sites for the coupling protein and the reductase, which are consistent with the cross-linking data, the fluorescence data, and the EXAFS and EPR spectral effects observed in the presence of the coupling protein. There is a wide canyon formed by the $\alpha\beta$ pairs in the dimer (Figure 4). Two of the iron-binding helices are exposed in this canyon and could interact with the coupling protein, resulting in a conformational change near the active site. Two of the iron ligands, Glu209 and Glu243, are particularly well located to be affected by this type of interaction. The changes observed in the EPR and EXAFS spectra of the hydroxylase could reflect altered coordination of these ligands, perhaps as described by a carboxylate shift mechanism.[58] Since optimal activity of the hydroxylase requires 2 mol of coupling protein,[33] it is probable that there are two binding domains for this component, located in the two canyons related by the noncrystallographic

(55) Valentine, A. M.; Lippard, S. J. Unpublished results.

(56) Bufford, H.; Rosenzweig, A. C.; Hedman, B.; Lippard, S. J.; Hodgson, K. O. Unpublished results.

(57) Feig, A. L.; Lippard, S. J. *Chem. Rev.* **1994**, *94*, 759−805.

(58) Rardin, R. L.; Tolman, W. B.; Lippard, S. J. *New J. Chem.* **1991**, *15*, 417−430.

2-fold axis. The canyon is large enough to accommodate the reductase as well, in the region closer to the β subunit. Similarly, there are probably two binding domains for the reductase, located on opposite faces of the molecule. The possible binding sites for the reductase and coupling protein are shown schematically in Figure 5. There are a several tryptophan residues in the canyon, some of which are good candidates for fluorescence quenching by reductase binding.

Conclusions and Unsolved Mysteries

Many features of the hydroxylase structure were accurately predicted from spectroscopic, biochemical, and model-building techniques. Some aspects of the structure were not predetermined, however. For example, an exogenous bridging acetate ligand, probably introduced via the crystallization buffer, was unexpected. The binding of anions such as fluoride,[59] azide,[39] and phenoxide[60] to the oxidized hydroxylase has been reported. If the acetate is derived from the crystallization buffers, another bridging ligand may be present in the native oxidized hydroxylase. One possibility is a second hydroxo bridge, but the Fe···Fe distance of 3.4 Å from both the EXAFS analysis and the crystal structure is too long to be consistent with the presence of two hydroxo bridges. Perhaps a similar exogenous bridging ligand is present in the native hydroxylase active site, for example, formate ion. Formate is produced from methanol in a later step in the metabolic pathway of methanotrophic bacteria and could serve a regulatory role. Further experiments are required to test such a hypothesis. In addition, details of the secondary structure, the striking similarity between the folds of the α and β subunits, the geometric features of the diiron center, including the coordination modes of the two histidine and four glutamate ligands, hydrogen-bonding interactions among ligands in the coordination spheres, the coordination sites of the bridging hydroxide and terminal water ligands, and the specific amino acid residues involved in subunit interactions, were completely new revelations, as were other aspects of the protein structure reported in more detail elsewhere.[25] The information contained in the structure, which could not have been obtained by other methods, suggests an array of exciting new experiments which will help us further to understand this amazing and complex multicomponent enzyme system.

This work was supported by grants from the National Institute of General Medical Sciences and Shell Research BV.

(59) Hamman, S.; Atta, M.; Ehrenberg, A.; Wilkins, P.; Dalton, H.; Béguin, C.; Fontecave, M. *Biochem. Biophys. Res. Commun.* **1993**, *195*, 594–599.

(60) Andersson, K. K.; Elgren, T. E.; Que, L., Jr.; Lipscomb, J. D. *J. Am. Chem. Soc.* **1992**, *114*, 8711–8713.